

Pauli Virtanen and Tero T. Heikkilä. 2007. Peltier effects in Andreev interferometers. Physical Review B, volume 75, number 10, 104517.

© 2007 American Physical Society

Reprinted with permission.

Readers may view, browse, and/or download material for temporary copying purposes only, provided these uses are for noncommercial personal purposes. Except as provided by law, this material may not be further reproduced, distributed, transmitted, modified, adapted, performed, displayed, published, or sold in whole or part, without prior written permission from the American Physical Society.

<http://link.aps.org/abstract/prb/v75/e104517>

Peltier effects in Andreev interferometers

Pauli Virtanen* and Tero T. Heikkilä†

Low Temperature Laboratory, Helsinki University of Technology, P.O. Box 2200 FIN-02015 TKK, Finland

(Received 8 December 2006; revised manuscript received 14 February 2007; published 29 March 2007)

The superconducting proximity effect is known to modify transport properties of hybrid normal-superconducting structures. In addition to changing electrical and thermal transport separately, it alters the thermoelectric effects. Changes to one off-diagonal element L_{12} of the thermoelectric matrix L have previously been studied via the thermopower, but the remaining coefficient L_{21} , which is responsible for the Peltier effect, has received less attention. We discuss symmetry relations between L_{21} and L_{12} in addition to the Onsager reciprocity, and calculate Peltier coefficients for a specific structure. Similar to the thermopower, for finite phase differences of the superconducting order parameter, the proximity effect creates a Peltier effect significantly larger than the one present in purely normal-metal structures. This results from the fact that a nonequilibrium supercurrent carries energy.

DOI: 10.1103/PhysRevB.75.104517

PACS number(s): 74.25.Fy, 73.23.-b, 74.45.+c

In large metallic structures, linear-response transport can be described using the thermoelectric matrix L that relates charge and energy currents to temperature and potential biases.¹ The off-diagonal coefficients describe coupling between heat and charge currents and indicate the magnitude of the thermopower and the Peltier effect. In many cases, these coefficients are coupled by Onsager's reciprocal relation $L_{\alpha\beta}(B) = L_{\beta\alpha}(-B)$ under the reversal of the magnetic field B .^{1,2}

In hybrid normal-superconducting systems (see Fig. 1), the Cooper pair amplitude penetrates to the normal-metal parts. This makes the linear-response coefficients L different from their normal-state values and allows supercurrents $I_{S,\text{eq}}$ to flow through the normal metal even at equilibrium. The charge and energy (entropy) currents I_c^i and I_E^i entering different terminals can, in linear response, be written as

$$\begin{pmatrix} I_c^i - I_{S,\text{eq}}^i \\ I_E^i \end{pmatrix} = \sum_{j \in \text{terminals}} \begin{pmatrix} L_{11}^{ij} & L_{12}^{ij} \\ L_{21}^{ij} & L_{22}^{ij} \end{pmatrix} \begin{pmatrix} \Delta V_j \\ \Delta T_j / \bar{T} \end{pmatrix}, \quad (1)$$

in terms of the biases $\Delta V_j = V_j - \bar{V}$, $\Delta T_j = T_j - \bar{T}$, and the modified response coefficients L . The proximity-induced changes in the conductance L_{11}^{ij} ,^{3,4} thermal conductance L_{22}^{ij} / \bar{T} (for $L_{12}^{ij} = L_{21}^{ij} = 0$),⁴⁻⁷ and thermopower $-L_{12}^{ij} / (\bar{T} L_{11}^{ij})$ (Refs. 4 and 8-17) have recently been investigated both experimentally and theoretically. The behavior of the remaining off-diagonal coefficient L_{21}^{ij} has previously been discussed in Ref. 4 using scattering theory, but the simulations were restricted to small structures—making the contribution from electron-hole asymmetry very large.

In this paper, we note that within reasonable approximations, in diffusive superconducting heterostructures Eq. (1) can be generalized to the nonlinear regime by defining an energy-dependent thermoelectric matrix $\tilde{L}_{\alpha\beta}^{ij}(E)$. We show that this quantity satisfies an Onsager reciprocal relation $\tilde{L}_{\alpha\beta}^{ij}(E, B) = \tilde{L}_{\beta\alpha}^{ji}(E, -B)$ under the reversal of the magnetic field B and the phase $\arg \Delta$ of the superconducting order parameter, whenever i and j refer to normal terminals. We also show how the proximity effect modifies L_{21} , giving rise

to a large Peltier effect,¹ and discuss how it could be experimentally detected.

Qualitatively, one can understand the origin of proximity-induced thermoelectric effects by noting that charge current consists of a quasiparticle component and a supercurrent component. That the latter is strongly temperature dependent in proximity structures then leads to a finite L_{12} coefficient,^{9,11} via a mechanism analogous to charge imbalance generation in superconductors.^{18,19} Assuming the Onsager symmetry, one would also expect that L_{21} is finite. The actual form of the coupling can be seen by inspecting the quasiclassical transport equations [Eqs. (4) below] or by studying their near-equilibrium approximation in a diffusive normal metal under the influence of a weak proximity effect (see, for example, Ref. 12):

$$\nabla \cdot J_c = 0, \quad \nabla \cdot J_E = 0, \quad (2a)$$

$$J_c = -\tilde{\sigma} \nabla \delta V + \tilde{T} \nabla \delta T + \frac{\partial J_{S,\text{eq}}}{\partial T} \delta T + J_{S,\text{eq}}, \quad (2b)$$

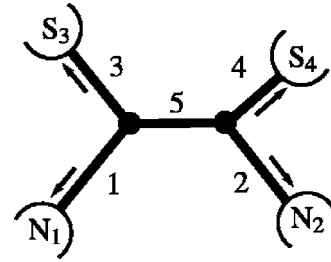


FIG. 1. Example of a four-probe structure considered in the text: five normal-metal wires connected to each other and to four terminals, of which two are superconducting (S) and two normal (N). We take the lengths l , cross-sectional areas A , and conductivities σ of the wires to be $l/l_0 = (1.5, 1, 1.2, 1, 0.8)$ and $A\sigma/A_0\sigma_0 = (0.8, 1, 0.8, 1, 1)$. Here, l_0 , A_0 , and σ_0 are some characteristic values controlling the energy scale $E_T = \hbar D / (l_3 + l_4 + l_5)^2$ of the proximity effect. The system is chosen so as to bring out effects that depend on the magnitude of geometrical asymmetry. In the numerics, all wires are assumed to be quasi-one-dimensional, $l \gg \sqrt{A}$.

$$J_E = -\tilde{\sigma}_{\text{th}} \nabla \delta T - \tilde{T} \nabla \delta V + \tilde{T} \frac{\partial J_{S,\text{eq}}}{\partial T} \delta V. \quad (2c)$$

Here, δV and δT are deviations of the (effective) local potential and temperature from equilibrium, and \bar{T} is the ambient temperature. The first terms in charge and energy current densities J_c and J_E can be considered the quasiparticle current and the rest the (nonequilibrium) supercurrent; $\tilde{\sigma}$ and $\tilde{\sigma}_{\text{th}}$ are the proximity-modified charge and thermal conductivities, $J_{S,\text{eq}}$ is the equilibrium supercurrent density, and \tilde{T} is a small factor associated with nonequilibrium supercurrent. Although Eqs. (2) are not of the usual form of normal-state transport equations,¹ one can see that a variation δT generates a change in the charge current, and that a nonequilibrium ($\delta V \neq 0$) supercurrent carries energy current. The corresponding response coefficients in Eqs. (2b) and (2c) are not independent, which is a signature of the Onsager symmetry. Comparing the magnitude of the coefficients, it turns out that at low temperatures a large part of the thermoelectric coupling indeed arises from the temperature dependence of $J_{S,\text{eq}}$. At high temperatures, where it vanishes exponentially, other sources become more important.^{10,12,13}

However, the validity of Eqs. (2) is somewhat restricted, since these equations are correct only in the linear response and to the first order in the proximity corrections, additionally assuming that the energy gap $|\Delta|$ of the nearby superconductors satisfies $k_B \bar{T} \ll |\Delta|$. For quantitative calculations of the multiterminal transport coefficients, and to evaluate the proximity-corrected coefficients in Eq. (2), we start from the full nonequilibrium formalism.

The superconducting proximity effect can be described using the quasiclassical BCS-Gor'kov theory.^{20,21} Here, we concentrate on diffusive normal-metal structures that are connected to superconducting and normal terminals, and neglect any inelastic scattering. The model then reduces to the Usadel equations,^{21,22} whose first part, the spectral equations, can in this case be written as

$$D \nabla^2 \theta = -2i(E + i0^+) \sinh \theta + \frac{v_S^2}{2D} \sinh(2\theta), \quad (3a)$$

$$\nabla \cdot (-v_S \sinh^2 \theta) = 0, \quad v_S \equiv D(\nabla \chi - 2e\mathbf{A}/\hbar). \quad (3b)$$

They describe the penetration of the superconducting pair amplitude $F = e^{i\chi} \sinh \theta$ into the normal metal. We denote the diffusion constant of the metal here by D , and the magnetic vector potential by \mathbf{A} . At clean contacts to bulk superconductors, the pairing angle is $\theta = \text{arctanh}(|\Delta|/E)$ and the phase $\chi = \arg \Delta$, where Δ is the superconducting order parameter. Transport properties are, in turn, determined by kinetic Boltzmann-like equations,

$$D \nabla \cdot \hat{\Gamma}_{Tf} = \mathcal{R} f_T + D(\nabla \cdot j_S) f_L, \quad D \nabla \cdot \hat{\Gamma}_{Lf} = 0, \quad (4a)$$

$$\hat{\Gamma}_{Tf} \equiv \mathcal{D}_T \nabla f_T + T \nabla f_L + j_S f_L, \quad (4b)$$

$$\hat{\Gamma}_{Lf} \equiv \mathcal{D}_L \nabla f_L - T \nabla f_T + j_S f_T, \quad (4c)$$

which describe the behavior of the antisymmetric and symmetric parts $f_L(E) \equiv f(\mu_S - E) - f(\mu_S + E)$ and $f_T(E) \equiv 1 - f(\mu_S - E) - f(\mu_S + E)$ of the electron distribution function. They are defined with respect to the potential of the superconductors, chosen below as $\mu_S = 0$. The spectral supercurrent j_S , the diffusion coefficients \mathcal{D}_L , \mathcal{D}_T , and \mathcal{T} , and the condensate sink term \mathcal{R} are functionals of θ and χ , having the symmetries $\mathcal{D}_{LT}(\chi) = \mathcal{D}_{LT}(-\chi)$, $\mathcal{T}(\chi) = -\mathcal{T}(-\chi)$, $j_S(\chi) = -j_S(-\chi)$, and $\mathcal{R}(\chi) = \mathcal{R}(-\chi)$.^{12,21} In normal metals, $\nabla \cdot j_S = \mathcal{R} = 0$. Observable current densities are finally related to the spectral currents $\hat{\Gamma}_{LTf}$ through

$$J_c = -\frac{\sigma}{2|e|} \int_{-\infty}^{\infty} dE \hat{\Gamma}_{Tf}, \quad J_E = \frac{\sigma}{2e^2} \int_{-\infty}^{\infty} dE E \hat{\Gamma}_{Lf}, \quad (5)$$

and the heat current density is $J_Q = J_E - V J_c$ at the terminals. Below, we also assume that all contacts to terminals are clean and of negligible resistance: in this case, all quantities are continuous at the interfaces, except at superconductors since for $E < |\Delta|$ the boundary condition for the kinetic L mode is changed to $\hat{\mathbf{n}} \cdot \hat{\Gamma}_{Lf} = 0$, where $\hat{\mathbf{n}}$ is the normal to the interface.

It is important to note that the last two terms in Eqs. (4) mix the L and T modes and cause thermoelectric effects: near equilibrium, they lead to the coupling terms in Eqs. (2). Away from linear response, a nonequilibrium modification of the distribution function f due to the mixing²³ has also been experimentally observed in Ref. 24.

The aim in the following is to calculate the thermoelectric coefficients $L_{\alpha\beta}^{ij}$ starting from Eqs. (4). However, as with the charge conductance, it is useful to first define corresponding energy-dependent thermoelectric coefficients $\tilde{L}_{\alpha\beta}^{ij}(E)$. Since the kinetic equations are linear, it is possible to write the currents entering different terminals as

$$I_c^i = \int_{-\infty}^{\infty} dE \sum_{\beta j} \tilde{L}_{T\beta}^{ij}(E) f_{\beta}^j(E), \quad (6a)$$

$$I_E^i = \int_{-\infty}^{\infty} dE E \sum_{\beta j} \tilde{L}_{L\beta}^{ij}(E) f_{\beta}^j(E), \quad (6b)$$

where $\beta \in \{T, L\}$, j runs over all terminals, and f_{α}^j is the α -mode distribution function in terminal j . This spectral thermoelectric matrix $\tilde{L}_{\alpha\beta}^{ij}(E)$ is the quasiclassical counterpart of the P matrix in Ref. 4. More explicitly, $\tilde{L}_{\alpha\beta}^{ij}(E)$ can be defined as the α -mode current seen in terminal i that a unit excitation of mode β in terminal j generates at energy E :

$$\tilde{L}_{\alpha\beta}^{ij}(E) \equiv \int_{S_i} dS \hat{\mathbf{n}} \cdot \hat{\Gamma}_{\alpha} \psi^{j,\beta}. \quad (7)$$

Here, S_i is the surface of terminal i and $\hat{\mathbf{n}}$ the corresponding normal vector. The two-component function $\psi^{j,\beta}$ is assumed to satisfy the kinetic equations (4) with the electron distribution functions f_{α}^i in terminals replaced by $\delta_{\alpha\beta} \delta_{ij}$. The linear-response coefficients L are directly related to $\tilde{L}(E)$ via Eq.

(6), for example, $L_{11} = \frac{1}{2k_B T} \int dE \tilde{L}_{TT}(E) \text{sech}^2\left(\frac{E}{2k_B T}\right)$ and $L_{21} = \frac{-1}{2k_B T} \int dE E \tilde{L}_{LT}(E) \text{sech}^2\left(\frac{E}{2k_B T}\right)$.

The spectral thermoelectric matrix depends only on θ and χ , but not on the distribution functions at the terminals. Knowing the energy dependence of this matrix, one can directly evaluate currents also away from linear response, if changes in the order parameter Δ and any inelastic scattering can be neglected. The matrix $\tilde{L}_{\alpha\beta}^{ij}(E)$ is also possible to evaluate numerically once θ and χ have been solved, and it offers a feasible way of finding the response of the circuit to different types of excitations in the terminals.

An Onsager reciprocal relation for $\tilde{L}_{\alpha\beta}^{ij}(E)$ follows from the fact that the differential operator $\hat{\mathcal{L}}$ in Eqs. (4), $\hat{\mathcal{L}}f=0$, has the property

$$\hat{\mathcal{L}}(B)^\dagger = (-\nabla) \cdot \begin{pmatrix} \mathcal{D}_T & \mathcal{T} \\ -\mathcal{T} & \mathcal{D}_L \end{pmatrix}^\dagger (-\nabla) + (-\nabla) \cdot \begin{pmatrix} 0 & j_S \\ j_S & 0 \end{pmatrix}^\dagger - \begin{pmatrix} \mathcal{R} & -D(\nabla \cdot j_S) \\ 0 & 0 \end{pmatrix} = \hat{\mathcal{L}}(-B), \quad (8)$$

due to the symmetries of the coefficients under reversal of the phases χ , $\arg \Delta$, and the magnetic field B . Below, whenever we discuss the reversal of B , a reversal of the phases is also implied. Straightforward integration by parts now shows that for any volume Ω and two-component functions ϕ and ψ , we can write

$$\int_{\Omega} d\mathcal{V} [\psi^\dagger \hat{\mathcal{L}}\phi - \phi^\dagger \hat{\mathcal{L}}\psi] = \int_{\partial\Omega} dS \hat{\mathbf{n}} \cdot \mathbf{J}, \quad (9)$$

where $\partial\Omega$ is the boundary of Ω . For the differential operator here, the flux $J = \psi^\dagger \hat{\Gamma}(B)\phi - \phi^\dagger \hat{\Gamma}(-B)\psi - j_S \psi^\dagger \sigma_1 \psi$, σ_1 being the first spin matrix. Now, we choose Ω to be the whole conductor, with ϕ and ψ such that $\phi = \psi^{j,\beta}$ satisfies the conditions in the calculation for $\tilde{L}_{\alpha\beta}^{ij}(E, B)$ and $\psi = \psi^{i,\alpha}$ the conditions for $\tilde{L}_{\beta\alpha}^{ji}(E, -B)$. When both i and j refer to normal terminals, we then find

$$0 = \int_{\partial\Omega} dS \hat{\mathbf{n}} \cdot \mathbf{J} = \int_{S_i} dS \hat{\mathbf{n}} \cdot \hat{\Gamma}_\alpha(B)\phi - \int_{S_j} dS \hat{\mathbf{n}} \cdot \hat{\Gamma}_\beta(-B)\psi \quad (10)$$

using the boundary conditions imposed on ϕ and ψ and the fact that $j_S=0$ at normal terminals. Comparison of Eqs. (10) and (7) reveals a reciprocal relation,

$$\tilde{L}_{\alpha\beta}^{ij}(E, B) = \tilde{L}_{\beta\alpha}^{ji}(E, -B). \quad (11)$$

This implies that phase differences in the order parameter will be similar sources for quasiclassical Peltier and Thompson effects as they are for the thermopower discussed in Refs. 9–13. Similar relations exist also in the scattering theory.⁴

The form of Eqs. (6) also implies that $\tilde{L}(E, B)$ has the symmetries

$$\sum_j \tilde{L}_{TL}^{ij}(E) = 0 \quad \text{for normal terminal } i, \quad (12a)$$

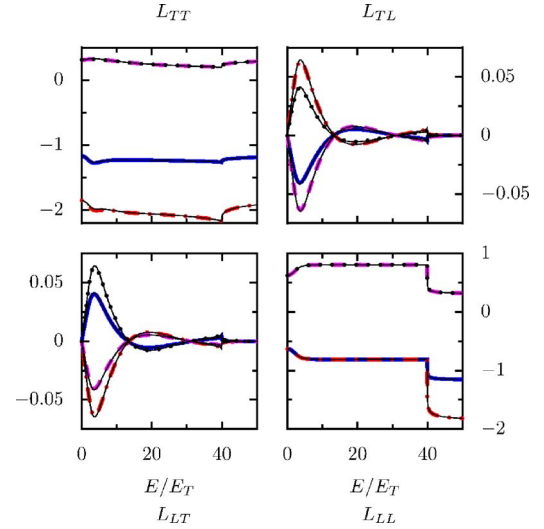


FIG. 2. (Color online) Elements $L_{\alpha\beta}^{ij}$ for $i, j=1,2$ and $\alpha, \beta=L, T$ for the asymmetric interferometer in Fig. 1, in units of $1/R_2$. The order parameters in the superconducting terminals have $\arg \Delta_3 - \arg \Delta_4 = 0.54\pi$ and $|\Delta_3| = |\Delta_4| = 40E_T$. The thick blue solid line is L^{11} , the dash-dotted red line L^{22} , the black dotted line L^{12} , and the magenta dashed line L^{21} . Note the symmetry $\tilde{L}_{\alpha\beta}^{ij}(E) = (-1)^{1-\delta_{\alpha\beta}} \tilde{L}_{\beta\alpha}^{ji}(E)$. Approximations found by solving Eqs. (4) to first order in j_S and \mathcal{T} are shown as thin solid lines—in general, they are indistinguishable from the exact numerical results.

$$\sum_j \tilde{L}_{LL}^{ij}(E) = 0, \quad (12b)$$

$$\tilde{L}_{\alpha\beta}^{ij}(E, -B) = (-1)^{1-\delta_{\alpha\beta}} \tilde{L}_{\alpha\beta}^{ij}(E, B), \quad (12c)$$

since the charge current to any normal terminal and the entropy current to any terminal must vanish at equilibrium for all temperatures. Equation (12c) follows essentially from the electron-hole symmetry assumed in the quasiclassical theory, leading to $\hat{\Gamma}_{Lf} \mapsto \hat{\Gamma}_{Lf}$, $\hat{\Gamma}_{Tf} \mapsto -\hat{\Gamma}_{Tf}$ under the transformations $B \mapsto -B$, $f_T \mapsto -f_T$.¹² This makes the diagonal coefficients symmetric in B and the off-diagonal ones antisymmetric. However, there are some experimental results^{8,14} where the latter symmetry does not hold. Such observations cannot be explained with the quasiclassical theory applied here.

Consider now the application of the formulation above in the structure in Fig. 1. We solve the spectral equations (3) in this structure numerically and calculate the spectral thermoelectric matrix from the solutions. The behavior of the two coefficients important for thermoelectric effects, spectral supercurrent j_S and the coefficient \mathcal{T} , is discussed for structures of this type, for example, in Refs. 12 and 25. Resulting elements of $L_{\alpha\beta}^{ij}(E)$ are plotted as a function of E in Fig. 2—the energy scale is given by the Thouless energy $E_T = \hbar D / (l_3 + l_4 + l_5)^2$. The diagonal elements $\tilde{L}_{TT}(E)$ and $\tilde{L}_{LL}(E)$ are spectral charge and energy conductances.^{3,5} At $E > |\Delta|$, energy current can also enter the superconductor, which is visible as a rapid change in the \tilde{L}_{LL} coefficient. The off-diagonal coefficients qualitatively follow the energy dependence of the spectral supercurrent j_S , which gives the most visible contri-

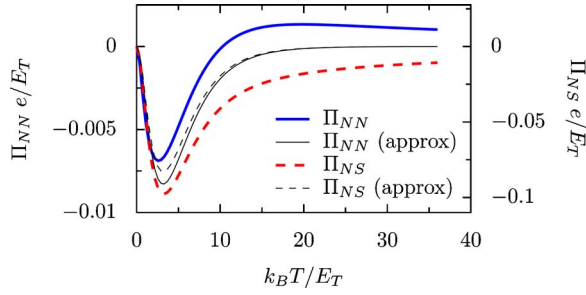


FIG. 3. (Color online) Peltier coefficients Π_{NN} and Π_{NS} for the same parameters as in Fig. 2. Approximations (14a) and (14b) are shown as thin lines—deviation from the exact result is due to neglecting T .

bution. Moreover, the elements of the matrix clearly exhibit symmetries (11) and (12).

The finite coefficient $\tilde{L}_{LT}^{ij}(E)$ leads to a Peltier effect: assume that the terminals are at a constant temperature $T^i = \bar{T}$ and biased at potentials chosen so that a current I_c flows between terminals 1 and 2, $I_c^1 = -I_c^2 = I_c$. Then, the Peltier linear-response coefficient for this system is

$$\Pi_{NN} \equiv \frac{dI_Q^1}{dI_c^1} = \frac{dI_E^1}{dI_c^1} = \frac{L_{21}^{11}W_1 - L_{21}^{12}W_2}{L_{11}^{11}W_1 - L_{11}^{12}W_2}, \quad (13)$$

where $W_j \equiv (L_{11}^{1j} + L_{11}^{2j})^{-1}$. We can also define the Peltier coefficient $\Pi_{NS} \equiv \frac{1}{2} dI_E^1 / dI_c^1$ corresponding to the current configuration $I_c^1 = I_c^2 = I_c / 2$.

The magnitude and temperature dependence of Π are shown in Fig. 3. For a typical Thouless energy of $E_T = 200 \text{ mK} k_B$ of an Andreev interferometer, the Peltier coefficients would be $|\Pi_{NN}| \sim 100 \text{ nV}$ and $|\Pi_{NS}| \sim 1 \mu\text{V}$ at $T \sim 200 \text{ mK}$. For comparison, Peltier coefficients for purely normal-metal junctions at these temperatures are of the order $\Pi = T(S^B - S^A) \sim 0.2 \text{ K} \times 10 \text{ nV/K} = 2 \text{ nV}$. The interferometer induces a significantly larger Π .

The above Peltier effect is related to the thermopower discussed in Refs. 9 and 11. We indeed find the Kelvin relations $\Pi_{NN} = TS_{NN}$ and $\Pi_{NS} = TS_{NS}$, which follow from the Onsager symmetry. Similar to Ref. 12, within the assumptions where Eqs. (2) apply, one can also find simple approximations up to first order in j_S :

$$\Pi_{NN} \approx \frac{(R_3 - R_4)R_5^2}{2(R_1 + R_2 + R_5)(R_3 + R_4 + R_5)} \frac{k_B T}{e} \frac{dI_{S,\text{eq}}}{dT}, \quad (14a)$$

$$\Pi_{NS} \approx \frac{4R_3R_4R_5 + R_5^2(R_3 + R_4)}{4(R_1 + R_2 + R_5)(R_3 + R_4 + R_5)} \frac{k_B T}{e} \frac{dI_{S,\text{eq}}}{dT}. \quad (14b)$$

Here, $I_{S,\text{eq}} \equiv \frac{A\sigma}{2} \int_{-\infty}^{\infty} dE j_S \tanh \frac{E}{2k_B T}$ is the equilibrium supercurrent. The above also shows the dependence on the asymmetry for Π_{NN} and the proportionality to the supercurrent—for this contribution to the effect.

Finite Peltier coefficients allow for cooling one of the

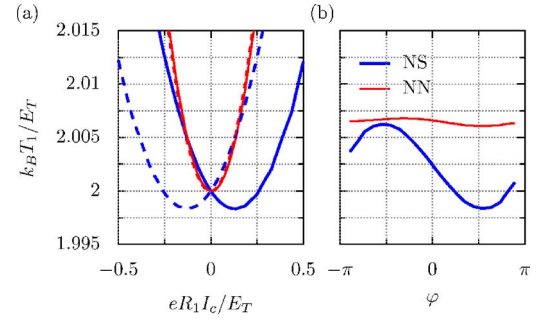


FIG. 4. (Color online) (a) Temperature of terminal 1 in Fig. 1 for $\varphi = \arg \Delta_3 - \arg \Delta_4 = \pm 0.54\pi$ (dashed and solid lines) and current configurations corresponding to Π_{NN} and Π_{NS} (red and blue lines) as a function of I_c . (b) T_1 for $eR_1 I_c / E_T = 0.15$ as a function of φ . The results are calculated assuming other terminals are at the temperature $T = 2E_T / k_B$. Deviation of T_1 from T originates from Joule heating and the oscillation of the proximity-Peltier effect.

terminals by driving electric current. Assume that the terminal is small enough such that the power flowing into the phonons is small compared to the heat current carried by electrons.^{7,26} The temperature change is then limited by the Joule heat generated in the wires: the heat current is $I_Q^1 = -G_{th} \Delta T_1 - 2\Pi_{NS} I_c^1 + e(I_c^1)^2 / G$, G and G_{th} being electrical and heat conductances. The maximum cooling effect then is, in a rough estimate assuming that the Wiedemann-Franz law applies, $\Delta T_1 = -(3/\pi^2)(e^2 \Pi_{NS}^2 / k_B T) / k_B \sim -0.3 \text{ mK}$ for $E_T = 200 \text{ mK} k_B$. Numerical calculation in the structure of Fig. 1 yields cooling $\Delta T \sim -0.4 \text{ mK}$, as shown in Fig. 4.

One point to note is that the B -symmetric oscillation of the thermal conductance^{5,6} also contributes to the temperature change, although this is significant only at temperatures small compared to E_T / k_B . In the absence of the Peltier effect, ΔT would hence be symmetric in B and always positive. The proximity-Peltier effect allows negative temperature changes and also breaks the symmetry, which makes the antisymmetric part $T_1(B) - T_1(-B)$ the experimentally interesting signal. In the structure in Fig. 1, the oscillation amplitude can be of the order of 1 mK for $E_T = 200 \text{ mK} k_B$ [see Fig. 4(b)]. Temperature changes of this order can be experimentally resolved in mesoscopic structures²⁶ so that the detection of the effect simply via observing ΔT should be experimentally viable. In addition to the off-diagonal thermoelectric coefficients L_{12} and L_{21} , it would also be interesting to study the Onsager reciprocity for $\tilde{L}_{TT}^{ij}(E)$ via differential conductances in multi-terminal structures.

In summary, we have studied charge and energy transport and its symmetry relations in normal-superconducting hybrid structures. We show that a large Peltier effect controlled by the phase difference over a Josephson junction can arise, partly due to coflowing quasiparticle and supercurrents. This complements previous studies of a related effect in the thermopower.

This research was supported by the Finnish Cultural Foundation and the Academy of Finland. We thank M. Meschke and I. A. Sosnin for useful discussions.

*Electronic address: pauli.virtanen@tkk.fi

†Electronic address: tero.t.heikkila@tkk.fi

¹H. B. Callen, Phys. Rev. **73**, 1349 (1948).

²L. Onsager, Phys. Rev. **37**, 405 (1931).

³P. Charlat, H. Courtois, Ph. Gandit, D. Mailly, A. F. Volkov, and B. Pannetier, Phys. Rev. Lett. **77**, 4950 (1996).

⁴N. R. Claughton and C. J. Lambert, Phys. Rev. B **53**, 6605 (1996).

⁵E. V. Bezuglyi and V. Vinokur, Phys. Rev. Lett. **91**, 137002 (2003).

⁶Z. Jiang and V. Chandrasekhar, Phys. Rev. Lett. **94**, 147002 (2005).

⁷Z. Jiang and V. Chandrasekhar, Phys. Rev. B **72**, 020502(R) (2005).

⁸J. Eom, C.-J. Chien, and V. Chandrasekhar, Phys. Rev. Lett. **81**, 437 (1998).

⁹R. Seviour and A. F. Volkov, Phys. Rev. B **62**, R6116 (2000).

¹⁰V. R. Kogan, V. V. Pavlovskii, and A. F. Volkov, Europhys. Lett. **59**, 875 (2002).

¹¹P. Virtanen and T. T. Heikkilä, Phys. Rev. Lett. **92**, 177004 (2004).

¹²P. Virtanen and T. T. Heikkilä, J. Low Temp. Phys. **136**, 401 (2004).

¹³A. F. Volkov and V. V. Pavlovskii, Phys. Rev. B **72**, 014529 (2005).

¹⁴Z. Jiang and V. Chandrasekhar, Chin. J. Phys. (Taipei) **43**, 693 (2005).

¹⁵A. Parsons, I. A. Sosnin, and V. T. Petrashov, Phys. Rev. B **67**, 140502(R) (2003).

¹⁶A. Parsons, I. A. Sosnin, and V. T. Petrashov, Physica E (Amsterdam) **18**, 316 (2003).

¹⁷F. Giazotto, T. T. Heikkilä, A. Luukanen, A. Savin, and J. Pekola, Rev. Mod. Phys. **78**, 217 (2006).

¹⁸A. Schmid and G. Schön, Phys. Rev. Lett. **43**, 793 (1979).

¹⁹C. J. Pethick and H. Smith, Phys. Rev. Lett. **43**, 640 (1979).

²⁰N. B. Kopnin, *Theory of Nonequilibrium Superconductivity*, International Series of Monographs on Physics No. 110 (Oxford University Press, Oxford, 2001).

²¹W. Belzig, F. K. Wilhelm, C. Bruder, G. Schön, and A. D. Zaikin, Superlattices Microstruct. **25**, 1251 (1999).

²²K. D. Usadel, Phys. Rev. Lett. **25**, 507 (1970).

²³T. T. Heikkilä, T. Vänskä, and F. K. Wilhelm, Phys. Rev. B **67**, 100502(R) (2003).

²⁴M. S. Crosser, P. Virtanen, T. T. Heikkilä, and N. O. Birge, Phys. Rev. Lett. **96**, 167004 (2006).

²⁵T. T. Heikkilä, J. Särkkä, and F. K. Wilhelm, Phys. Rev. B **66**, 184513 (2002).

²⁶M. Meschke, W. Guichard, and J. Pekola, Nature (London) **444**, 187 (2006).